

**Manuscript of the article: Reaction Kinetics, Mechanisms and Catalysis 110 (2013)  
53-62.**

**DOI: 10.1007/s11144-013-0584-z**

**A study of the selective hydroconversion of biocarboxylic acids to bioalcohols over novel  
indium-nickel/zeolite catalysts using octanoic acid as model reactant**

Szabolcs Harnos<sup>a,\*</sup>, György Onyestyák<sup>a</sup>, Szilvia Klébert, Magdalena Štolcová<sup>b</sup>, Alexander Kaszonyi<sup>b</sup> and József Valyon<sup>a</sup>

*<sup>a</sup>Institute of Materials and Environmental Chemistry, Research Centre for Natural Sciences, Hungarian Academy of Sciences, Pusztaszeri u. 59-67, Budapest, Hungary, H-1025*

*<sup>b</sup>Department of Organic Technology, Slovak University of Technology  
Radlinského 9, Bratislava, Slovak Republic, SK-81237*

**ABSTRACT**

Octanoic acid (OA) was hydrotreated in a flow-through reactor at 21 bar total pressure and 240-340 °C over supported metal catalysts prepared from Ni-zeolites (A, X, P) by indium modification. The Ni-zeolites were activated first in H<sub>2</sub> flow at 21 bar and 450 °C. While a fraction of the nickel got fully reduced the zeolite structure became partially destructed. However, some nickel cations remained unreduced and large fraction of the crystalline zeolite structure was retained. The indium modification of the reduced Ni-zeolites generated bimetallic NiIn/Ni<sub>H</sub>-zeolite catalysts having higher stability, hydroconversion activity, octanol selectivity, and lower hydrodecarbonylation activity than the parent partially destructed Ni-zeolite and the Adkins-type catalysts, commercially applied for the conversion of fatty acids to alcohols.

\*Corresponding author. E-mail: [harnos.szabolcs@ttk.mta.hu](mailto:harnos.szabolcs@ttk.mta.hu)

*Keywords:* Biomass, Fatty acids; Hydroconversion; Alcohols; NiIn/Ni,H-zeolites

## 1. Introduction

In the last decade, the research activity on the field of biomass conversion to chemicals and fuels has significantly increased as the necessity for the utilization of renewable carbon sources has become more evident. The renewable carbon sources are the carbon dioxide and the biomass, such as triglycerides (fats, vegetable oils), animal by-products, and organic wastes, predominantly lignocellulosic materials. Triglycerides are transesterified or hydroconverted to get fuel components. The primary degradative processing of other biomasses involves either gasification, or pyrolysis, hydrolysis, and/or fermentation. The pyro-oils or aqueous solutions obtained in mentioned processes usually give oxygen-rich organic compounds, referred to as platform molecules, which are valuable chemical intermediates. Among them mention must be made about the glycerol and fatty acids obtainable from triglyceride. Abundant platform intermediates are the carboxylic acids having 2 to 6 carbon atoms, including aliphatic mono and dicarboxylic acids, the oxo or hydroxy substituted derivatives thereof, and the furan mono and dicarboxylic acids [1]. The platform molecules have to be processed to get more valuable chemicals or fuel. In order to get quality fuels the oxygen content of these compounds must be reduced favorably in a catalytic process. Heterogeneous catalysts applying complex bi- or trimetallic catalysts seem to gain more and more significance in the biomass upgrading technologies [1-3]. Catalytic hydrodeoxygenation (HDO) is a plausible solution for upgrading oxygen-rich platform materials. The value of the HDO product strongly depends on the catalytic selectivity. For instance, HDO of short chain carboxylic acids can give either gaseous hydrocarbons or liquid phase alcohols, where latter is representing higher value as chemical or fuel component.

Recent studies concern the HDO of carboxylic acids over catalysts obtained by the reduction and In-modification of Cu-zeolites [4-8]. The crystalline structure of Al-rich Cu-

zeolites (A, X and P) completely collapsed upon H<sub>2</sub> reduction at temperature as low as 250 °C [4-7]. Nevertheless, the In-additive was found to suppress the total hydrogenation and decarboxylation, both resulting in hydrocarbons, and to promote alcohol formation. Added to Ni/Al<sub>2</sub>O<sub>3</sub> catalyst the indium proved to be even more efficient directing the reaction toward aliphatic alcohols [4, 9-10].

In contrast to Cu-zeolites the Ni-zeolites do not get fully reduced in H<sub>2</sub> even above the highest HDO temperature applied in the present study (360 °C). The residual nickel cations stabilize a relatively large fraction of the zeolite in crystalline form. The HDO properties of In-modified Ni-zeolite catalysts (NiIn/Ni,H-zeolite) were not studied yet. The aim of present work was to understand the relationship between the structure and the HDO activity of NiIn/Ni,H-zeolite catalysts using octanoic acid (OA) as model reactant.

## 2. Experimental

Nickel-zeolites (A, X, P) were prepared from NaA (Baylith), NaX (product of the late VEB CKB, Bitterfeld-Wolfen, Germany) and NaP (Crosfield Zeocross) powders, by conventional aqueous ion-exchange using nickel(II)acetate solution. The amount of Ni<sup>2+</sup> ions in the applied solution was about equivalent to the ion-exchange capacity of the zeolite. The preparations were designated as 13NiA, 11NiA, 10NiX, and 8NiP where the number gives the Ni content of the sample in weight percent. Bimetallic catalyst precursors were obtained by adding 10 wt.% indium(III)oxide to the Ni-zeolite and grinding the mixture in agate mortar. The catalysts prepared from the precursor by H<sub>2</sub>-reduction are designated as In13NiA, In11NiA, etc.

The XRD patterns of the catalysts were recorded by Philips PW 1810 diffractometer at elevated temperatures in hydrogen flow using a high temperature XRD cell (HT-XRD). The crystalline phases were identified using the ICDD database [11].

Nitrogen adsorption measurements were carried out at  $-196\text{ }^{\circ}\text{C}$  using Quantochrome Autosorb 1C instrument.

The catalytic hydrogenation of OA was carried out in a high-pressure fixed bed flow-through reactor at 21 bar total pressure in the temperature and space time (or WHSV) ranges of  $240\text{-}360\text{ }^{\circ}\text{C}$  and  $0.3\text{-}2\text{ h}$  (or  $0.5\text{-}3.3\text{ h}^{-1}$ ), respectively. Each catalyst precursor was reduced in hydrogen flow *in situ* in the reactor at  $450\text{ }^{\circ}\text{C}$  for 1 h in order to generate active supported metal prior to the catalytic test. The reactor effluent was cooled to room temperature and the liquid and gas phase products were separated. The liquid was analyzed by a gas chromatograph (GC, Shimadzu 2010) equipped with flame ionization detector and a CP-FFAP CB capillary column. The gas was analyzed by an on-line GC (HP 5890) equipped with thermal conductivity detector and Carboxen 1006 PLOT capillary column. The activity and the selectivity of the catalysts were characterized by product distributions represented by stacked area graphs. In this representation, the distance between two neighboring curves gives the yield of the specified product in weight percent.

For comparison a commercial Adkins catalyst (consisting of 72 wt.%  $\text{CuCr}_2\text{O}_4$  and 28 wt.%  $\text{CuO}$ ) was also tested applying the same activation and reaction conditions as for the catalysts of the present study.

### 3. Results and discussion

The applied NiA, NiX and NiP zeolites had about the same Si to Al ratio (near to 1) and therefore, similar chemical composition. Zeolites A and X are small ( $0.41\times 0.41\text{ nm}$ ) and large pore ( $0.74\times 0.74\text{ nm}$ ) structures built up from truncated octahedra interlinked by tetragonal and hexagonal prisms, respectively. The zeolite P having the framework structure of gismondite (GIS) has pores as narrow as  $0.45\times 0.31\text{ nm}$ .

The HT-XRD patterns, given in Fig. 1, show the transformation of the crystalline NiP phase and the  $\text{In}_2\text{O}_3/\text{NiP}$  phases upon treatment in  $\text{H}_2$  flow at 450 and 650 °C. The treatment of the NiP generates Ni metal particles (Fig. 1b,c) whereas  $\text{Ni}_2\text{In}$  intermetallic compound is formed in the preparation containing both  $\text{In}_2\text{O}_3$  and NiP (Fig. 1A,B,C).

All the admixed  $\text{In}_2\text{O}_3$  can be converted at this temperature to  $\text{In}^0$  and that can form immediately a new  $\text{Ni}_2\text{In}$  bimetallic phase (see in Fig. 1B and 1C). The  $\text{In}^0$  phase not consumed in the reaction with Ni would be detectable by XRD only below 156.6 °C, the melting temperature of indium metal. The intensity of the  $\text{Ni}_2\text{In}$  diffraction lines parallels the degree of nickel reduction that is higher after higher temperature  $\text{H}_2$  treatment (cf. Fig. 1b,B and 1c,C). Studies of the selective catalytic hydroconversion of carboxylic acids to alcohols suggest that the  $\text{Ni}_2\text{In}$  phase is responsible for the favorable catalytic effects [9-10].

Upon reduction reflections of the GIS structure became weaker and the GIS framework slightly expanded at the elevated temperature of the reduction as indicated by the somewhat higher  $2\Theta$  degrees of the residual reflections (Fig. 1). The intensity decrease of the diffraction lines from the GIS structure can indicate partial destruction of the zeolite structure upon reduction of the  $\text{Ni}^{2+}$  lattice cations. However, the changed scattering properties of the material because of the formation of nickel nanoparticles is a possible other reason of intensity change of zeolite reflections.

The reductive reaction of NiA or NiX is different from that of NiP. A large fraction of nickel cations in NiA and mainly in NiX cannot be reduced up to 450 °C. Consequently, the NiX hardly suffered structural destruction during reduction up to about 450 °C. The reductive conversion of the  $\text{NiX}/\text{In}_2\text{O}_3$  mixture did not generate XRD detectable  $\text{Ni}_2\text{In}$  phase, which can be only observed above 450 °C, at higher reduction degree of  $\text{Ni}^{2+}$  cations to metal in zeolites A.

The average nickel particle sizes, calculated by the Scherrer equation were found to be 30, 20 and 11 nm for the 10NiX, 13NiA and 8NiP catalysts, respectively. The same Ni particle sizes were obtained for the In-modified 8NiP sample.

It is to be mentioned that no bulk indium phase could be detected in any of the above described reduced Ni-zeolite/ $\text{In}_2\text{O}_3$  composites even below the melting temperature of  $\text{In}^0$ . That can indicate that the melt indium was perfectly dispersed in the pores and on the surface of the support and the nickel metal particles and the high dispersion was retained even at room temperature, where the indium phase must be solid.

As a conventional method the adsorption capacity of the micropores is used to draw conclusion about the zeolite content of zeolite-containing materials. The adsorption isotherms of Fig. 2 show that the adsorptive  $\text{N}_2$  molecules, having minimum cross sectional diameter of 0.364 nm, adsorbs mainly on the outer surface of the zeolite NaP crystallites. For this reason, no conclusion can be drawn about the degree of zeolite crystallinity from the low temperature  $\text{N}_2$  adsorption capacity of the narrow pore zeolites like zeolite A and P. Reduction of the  $\text{Ni}^{2+}$  lattice cations destabilizes the alumina-rich zeolite structure which can collapse in the vicinity of the reduced nickel. The zeolite NiA undergoes similar change upon reduction than the zeolite NiP. As a result the  $\text{N}_2$  uptake and the SSA of the narrow-pore zeolites increase upon partial destruction (Fig. 2). In contrast, the destruction of large pore zeolites, like the zeolite X, annihilates micropores, having high adsorption capacity at low pressure, and generates meso and macropores that have lower adsorption uptake at the same low pressure. Zeolite X has similar framework composition as zeolites A and P but its micropores are accessible for  $\text{N}_2$ . The  $\text{N}_2$  adsorption capacity of the zeolite NiX,  $\text{H}_2$  treated at 450 °C is commensurable to that of the NaX (223  $\text{cm}^3$  (STP)/g). Obviously, the NiX could preserve its structural integrity, because only a relatively small fraction of the nickel cations became reduced under the applied reduction conditions. This can apply also for zeolites NiP and NiA.

The facts that the  $\text{Ni}^{2+}$  zeolite was only partially reduced and the zeolite structure was mostly retained, while nickel particles were formed, which are much larger than the zeolite micropores, suggest that metal particles out of the crystallites are responsible for the catalytic effect of the material. The indium atoms on the surface of the supported nickel particles could provide bimetallic HDO sites, having similar catalytic properties as the supported  $\text{Ni}_2\text{In}$  phase.

The product distribution obtained using the bimetallic  $\text{In}_8\text{NiP}$  catalyst is significantly different of that obtained by the monometallic  $8\text{NiP}$  catalyst (Fig. 3A). Latter one shows fast activity decay. Using  $8\text{NiP}$  derived  $\text{In}_8\text{NiP}$  catalyst OA can be fully and selectively hydroconverted to octanol and this high activity and selectivity level can be maintained for at least 10 h time on stream (Fig. 3B). The stable activity was maintained also at somewhat lower temperature (Fig. 3C) except the appearance of some octanal that is the intermediate of octanol formation.

Fig. 4A shows the product distributions obtained over a commercial, conventionally used Adkins catalyst, having the composition of 72 wt.%  $\text{CuCr}_2\text{O}_4$  and 28 wt.%  $\text{CuO}$ , as a function of reaction temperature For comparison a figure was taken from an earlier study [9] to show the activity of an alumina-supported bimetallic  $\text{InNi}$  catalyst (Fig. 4B). The  $\text{InNi}$ /alumina catalyst was prepared using the same method applied for the preparation of the catalysts of the present study. The corresponding data for some catalysts of the present study are given in Figs. 4C to 4F. All the catalysts were able to produce alcohol from the fatty acid with high selectivity, but the chromium-free catalysts showed activity at lower temperatures and in narrower temperature range than the Adkins catalyst. Thus, the 80 % overall conversion of OA was attained already around 300 °C while on copper chromite only at 350 °C. Octanal is a characteristic intermediate reflecting the consecutive nature of the dominant reaction route. The octanal concentration in the product mixture can be reduced by using by increasing the reaction temperature or the space time (Figs. 4 and 5).

In contrast to the alumina supported catalyst the zeolite supported bimetallic catalysts were not active in bimolecular and monomolecular dehydration generating dioctyl ether and octane or octane, respectively.

In Fig. 6 the OA conversions were plotted against the reaction temperature to compare catalyst activities. The curves for the InNi/zeolite catalysts run between the conversion curves for the less active commercial Adkins catalysts and the most active InNi/alumina catalyst. The order of the catalyst activities is



The Ni nanoclusters in In8NiP have the average size of 10 nm the Ni particles in the NiIn/Al<sub>2</sub>O<sub>3</sub> catalyst have sizes near to 5-8 nm. In the In8NiP catalyst active metal surface has the highest whereas the support the lowest SSA. It is significant that the highest activity of NiIn/Al<sub>2</sub>O<sub>3</sub> catalyst is best approached by the In8NiP catalyst. The nanoparticle size seems to correlates with the activity. The idea that less damaged zeolite structure could be advantageous regarding the activity of the supported metal hydroconversion catalyst proved to be false. The surface of the NiIn nanoparticles must be chemically very similar resulting in very similar selectivities, whereas the dimension of this surface correlates with catalytic activity. The structure of the support can affect the size of metal nanoparticles.

#### 4. Conclusions

Indium-modified supported Ni catalysts has been discovered to be highly efficient for reduction of fatty acids by hydrogen. Hydrogen reduction of Ni-zeolites at 450 °C generates nickel particles on the outer surface of the zeolite crystallites. However, the Ni-zeolites become partially reduced and suffer only partial loss of crystallinity, if any. The indium modification of the Ni particles effectively promotes HDO of carboxylic acids to

alcolhols in consecutive steps and hinders mono- or bimolecular alcohol dehydration.

### **Acknowledgement**

The authors wish to express their appreciation to Mrs. Ágnes Farkas Wellisch for her technical assistance. Thanks is due to the Hungary-Slovakia Cross-border Co-operation Programme (Project registration number: HUSK/1101/1.2.1/0318) for supporting this research.

### **References**

- [1] Serrano-Ruiz JC, Luque R, Sepúlveda-Escribano A (2011) Chem Soc Rev 40: 5266-5281
- [2] **Centi G, Lanzafame P, Perathoner S (2012)** In: **Guczi L, Erdőhelyi A** (eds) Catalysis for Alternative Energy Generation, Springer, New York
- [3] Alonso DM, Wettstein SG, Dumesic J (2012) Chem Soc Rev 41: 8075-8098
- [4] Onyestyák Gy, Harnos Sz, Kalló D (2013) In: Woo HG, Choi HT (eds) Indium: Properties, Technological Applications and Health Issues, Nova Science Publishers, New York
- [5] Harnos Sz, Onyestyák Gy, Valyon J, Hegedűs M, Károly Z (2010) In: Derewinski M, Sulikowski B, Wegrzynowicz A (eds), Proceedings 10<sup>th</sup> Pannonian International Symposium on Catalysis, Polish Zeolite Association and Institute of Catalysis and Surface Chemistry, Krakow
- [6] Harnos Sz, Onyestyák Gy, Valyon J (2012), Appl Catal A 31: 439-440
- [7] Harnos Sz, Onyestyák Gy, Kalló D (2013) Micropor Mesopor Mater 167: 109-116

[8] Harnos Sz, Onyestyák Gy, Barthos R, Štolcová M, Kaszonyi A, Valyon J (2012) *Centr Eur J Chem* 10: 1954-1962

[9] Onyestyák Gy, Harnos Sz, Kalló D (2011) *Catal Com* 16: 184-188

[10] Harnos Sz, Onyestyák Gy, Barthos R, Štolcová M, Kaszonyi A, Kalló D (2012) *Catal Com* 27: 159-163

[11] B.D. Cullity (1978) In "Elements of X-ray Diffraction", 2<sup>nd</sup> edn. Addison-Wesley Publ Co. Reading, MA, USA

[12] Onyestyák Gy, Harnos Sz, Kalló D (2012) *Catal Com* 26: 19-24

## Figure captions

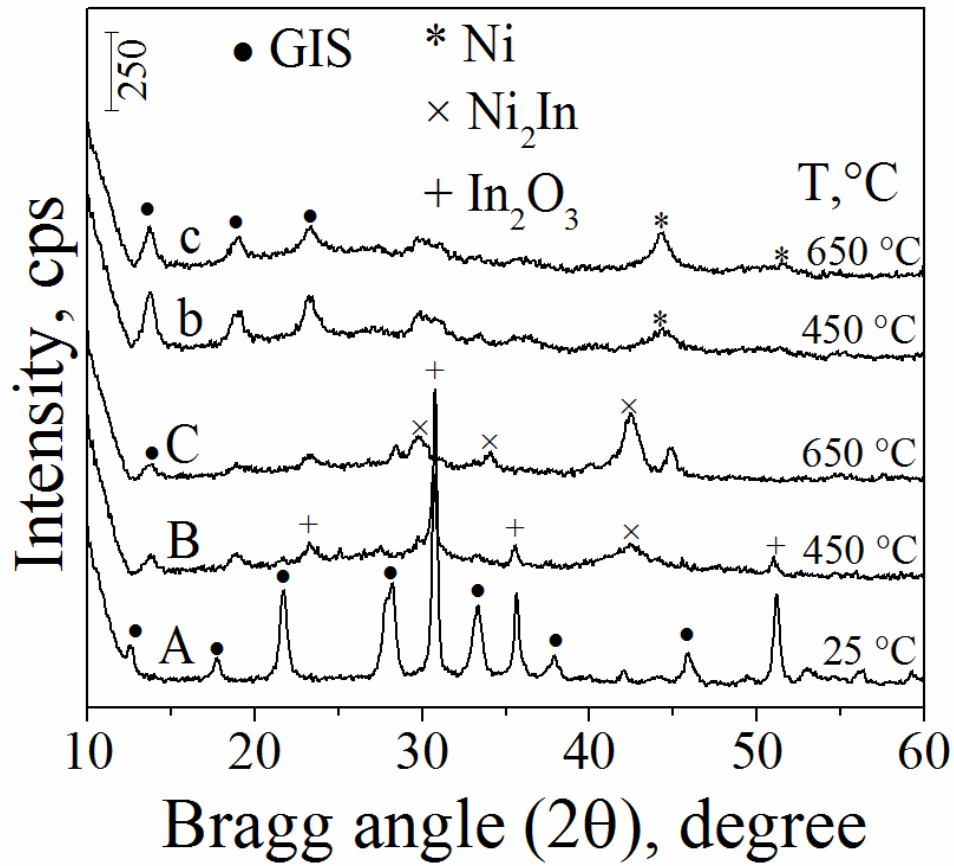


Fig. 1. HT-XRD patterns of the (b, c) indium free 8NiP catalysts and (A, B, C) 8NiP/10% In<sub>2</sub>O<sub>3</sub> mixtures, treated in H<sub>2</sub> flow for 30 min at (A) 25, (b, B) 450, and (c, C) 650 °C.

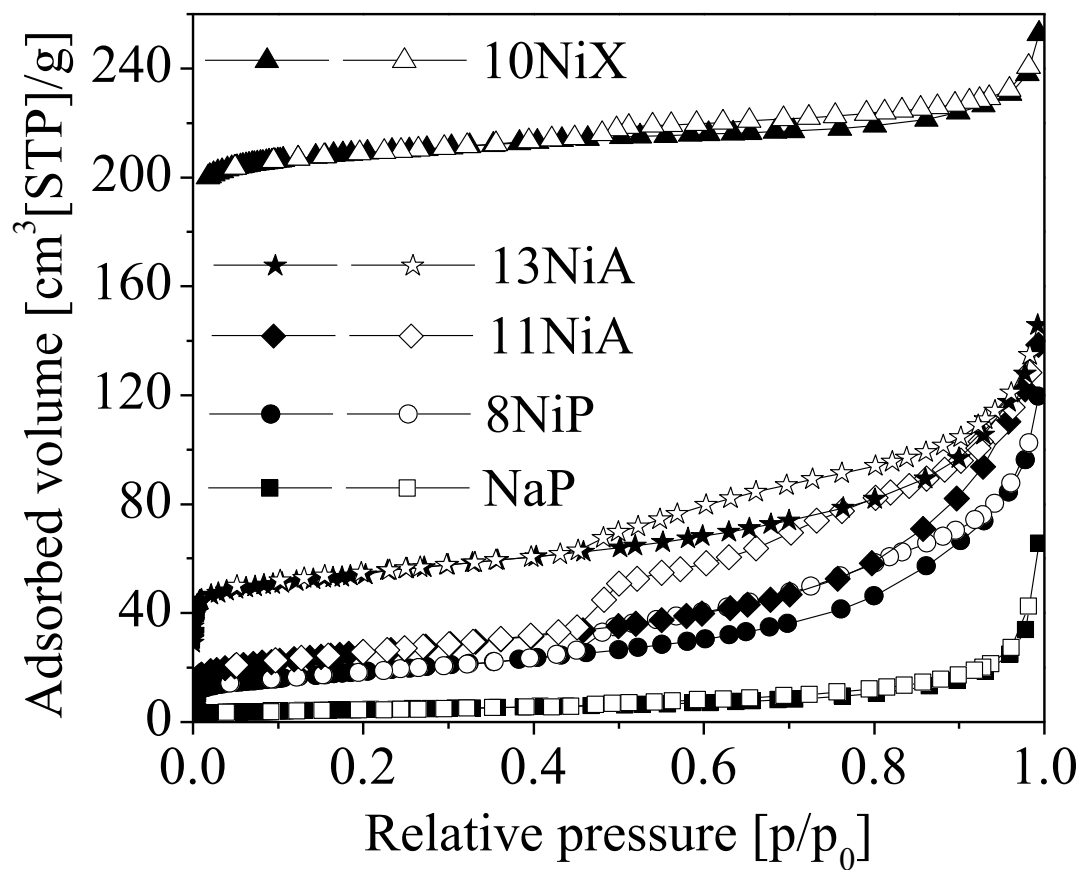


Fig. 2. Adsorption isotherms of nitrogen at -196 °C of parent NaP and NiP, reduced in H<sub>2</sub> flow at 450 °C. For comparison the isotherms are shown for reduced NiA and NiX samples.

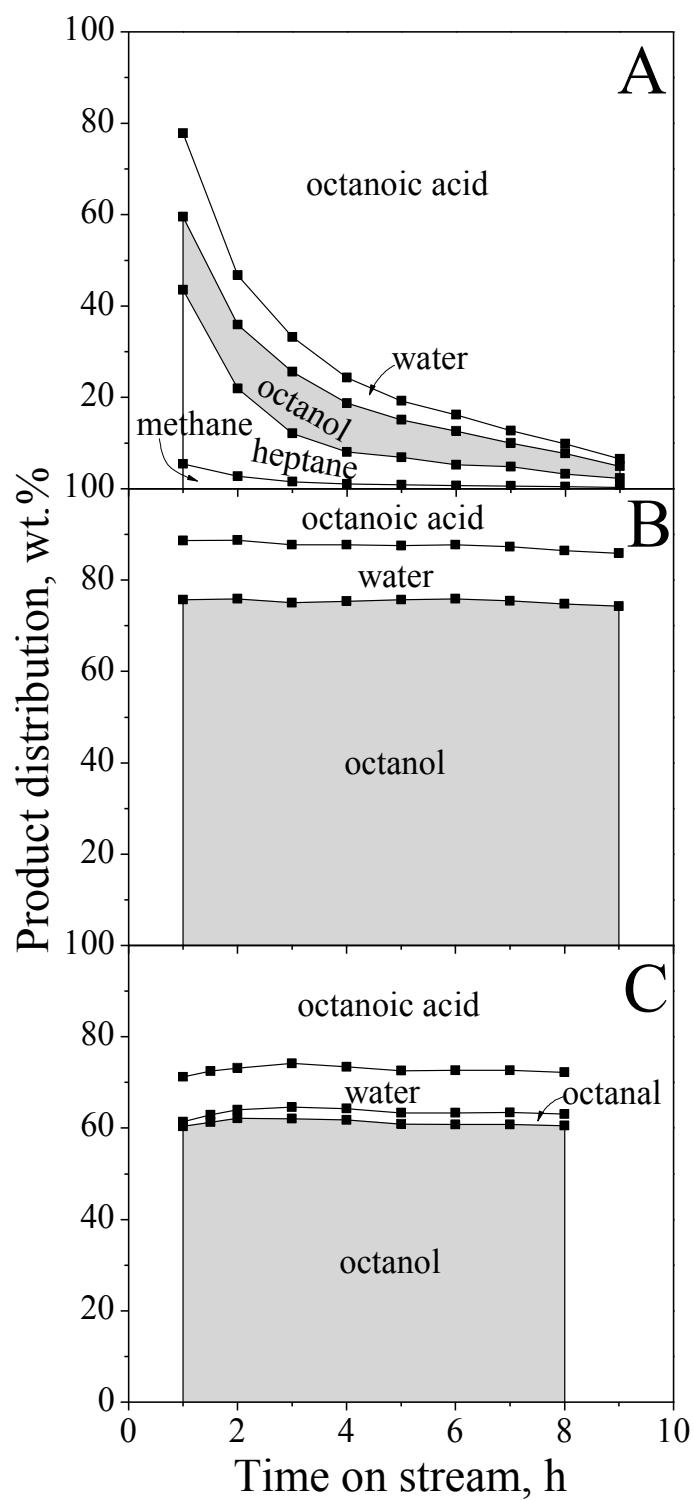


Fig. 3. Stacked area graphs of product distributions obtained from the hydroconversion of OA over catalysts (A) 8NiP at 300 °C, (B) In8NiP at 300 °C, and (C) In8NiP at 290 °C as a function of time on stream. The total pressure was 21 bar and the WHSV of OA was 2 h<sup>-1</sup>.

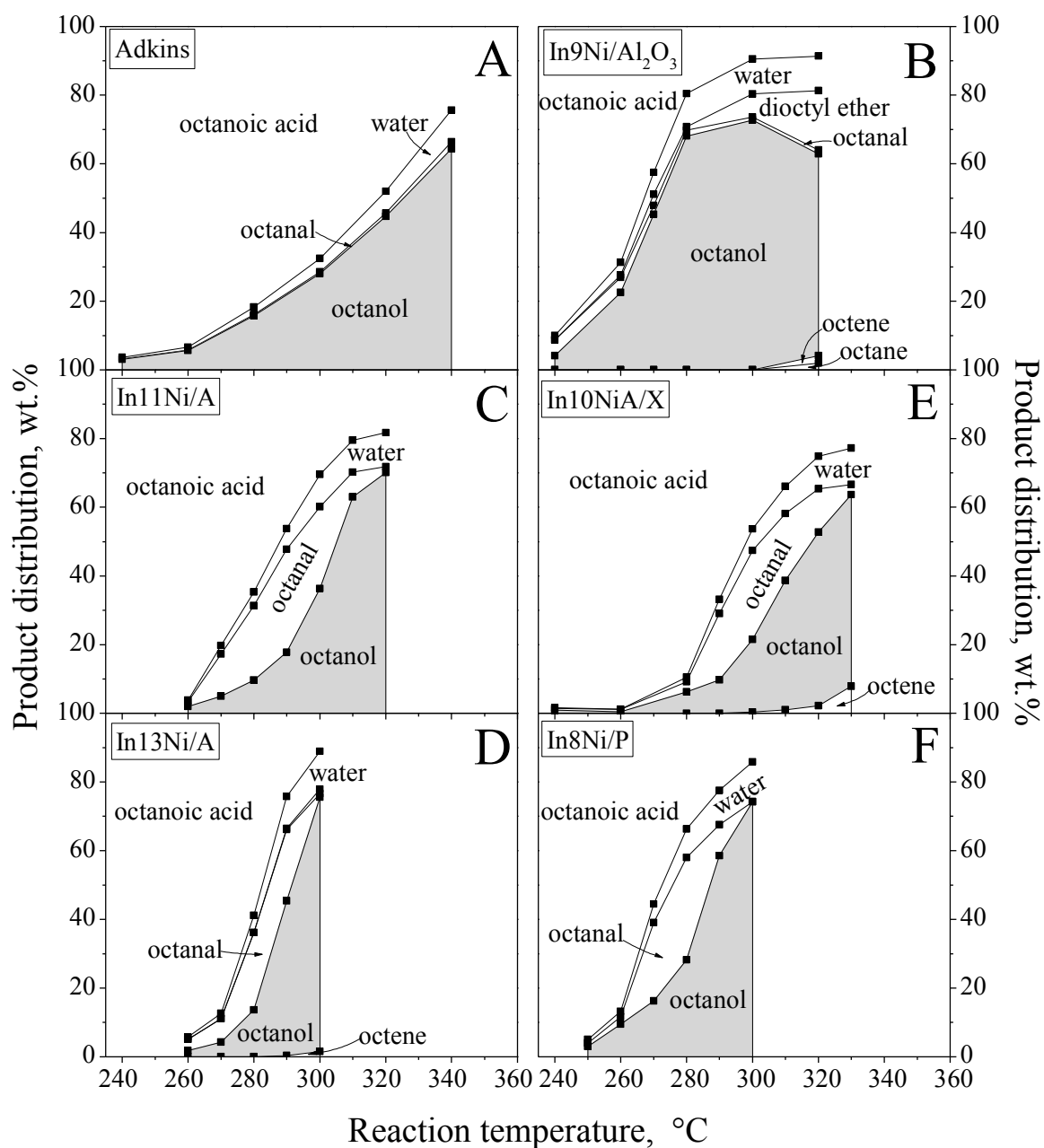


Fig. 4. Stacked area graphs of product distributions obtained from the hydroconversion of OA over catalysts (A) commercial Adkins, (B) In9Ni//Al<sub>2</sub>O<sub>3</sub> (C) In11NiA, (D) In13NiA, (E) In10NiX, and (F) In8NiP as a function of reaction temperature. The total pressure was 21 bar and the WHSV of OA was 2 h<sup>-1</sup>.

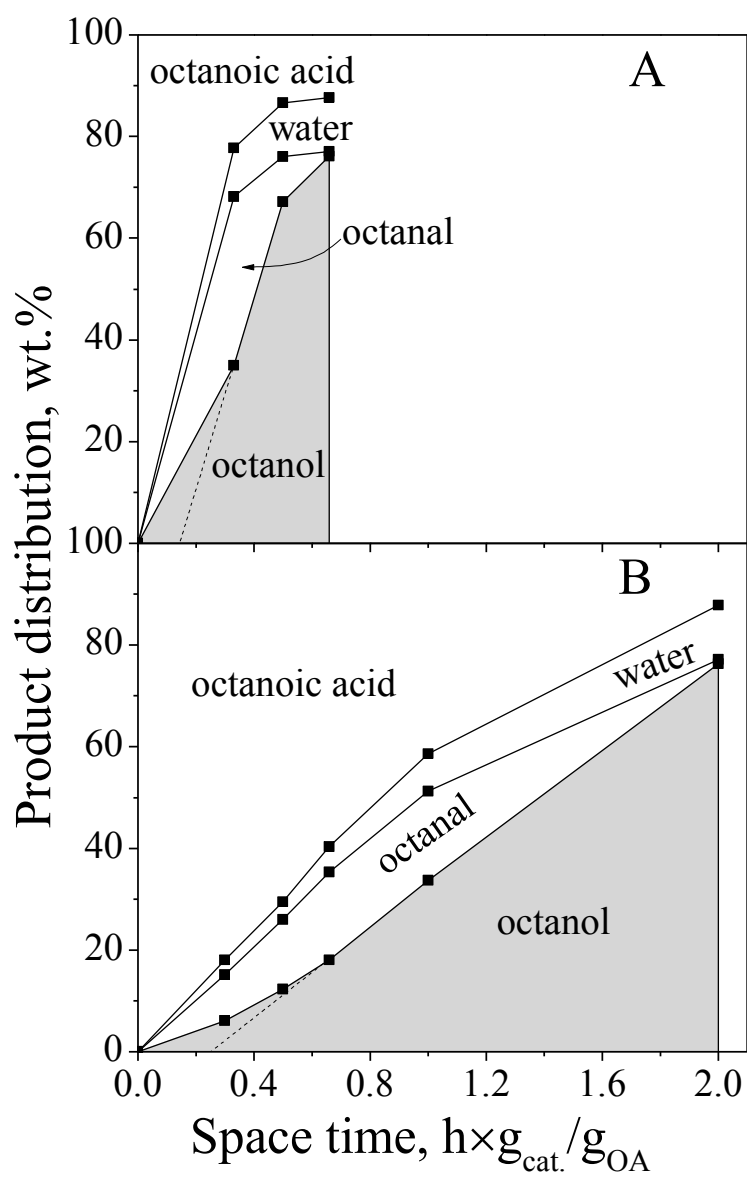


Fig. 5. Stacked area graphs of product distributions obtained from the hydroconversion of OA over catalyst In<sub>8</sub>NiP as a function of space time at 21 bar total and at temperature (A) 290 and (B) 270 °C.